Analytical Sciences (2023) 39:547–556
https://doi.org/10.1007/s44211-023-00267-y

ORIGINAL PAPER

A practical and rapid screening method for influenza virus neuraminidase inhibitors based on fluorescence detection

Junjie Xie[1] · Peng Tan[1] · Funeng Geng[2] · Qiang Shang[3] · Shanbo Qin[1] · Lu Hao[1]

Received: 10 November 2022 / Accepted: 29 December 2022 / Published online: 8 January 2023

Abstract

A new analytical method for rapid screening of influenza virus neuraminidase inhibitors was established. The method is based on the principle that, given a certain amount of neuraminidase, the sample and the neuraminidase act in the microplate for a period of time, and the active neuraminidase that is not inhibited by the sample can generate a fluorescence value at a specific wavelength after binding to the substrate, and the rate of inhibition of neuraminidase by the sample can be calculated based on the actual detected fluorescence value. This newly developed method was used to screen and evaluate the in vitro anti-neuraminidase activity of 39 high-purity compounds contained in three traditional Chinese herbal medicines, and finally 25 compounds with strong activity were obtained. The newly established neuraminidase inhibitor analytical method has these advantages of practicality, rapidity, high sensitivity and low cost, and has a good value for promotion and application.

Keywords Influenza virus neuraminidase inhibitor · Fluorescence detection · Traditional Chinese medicine · Molecular docking · Quality consistency

Introduction

Influenza (abbreviated as flu) is an acute respiratory infectious disease caused by influenza viruses, with seasonal epidemic characteristics or can be prevalent throughout the year, and the population is generally susceptible to infection, especially pregnant women, elderly people and patients with chronic diseases are prone to develop severe or critically ill cases, with a high risk of death, and have always posed a threat to public health [1–3]. It is particularly noteworthy that under the current COVID-19 epidemic, most patients with COVID-19 will present with influenza-like symptoms such as fever, dry cough, sore throat, and malaise at the initial stage of illness [4–6]. Influenza viruses are highly infectious and mutate rapidly [1, 7], and it is difficult to effectively prevent and control influenza through vaccination alone [8], and safe and effective drugs are still needed clinically as the ultimate treatment. The main classes of anti-flu drugs that have been marketed include M2 channel inhibitors and neuraminidase (abbreviated as NA) inhibitors, hemagglutinin inhibitors, and interferons. However, M2 channel inhibitors, such as amantadine, have serious neurotoxicity and are susceptible to drug resistance, so they are less commonly used in clinical practice. Although neuraminidase inhibitors, such as peramivir, oseltamivir, and zanamivir, can effectively inhibit NA to achieve anti-flu effects, they are not the optimal choice due to defects such as adverse effects [9, 10] and high price [11], so there is an urgent need to find other effective drugs. Therefore, the development of highly effective and low-toxicity anti-flu virus drugs is a major engineering and technical challenge.

Traditional Chinese medicine has been clinically used in China for thousands of years and has played an important role in the fight against major epidemics [12–14]. The screening of highly effective and low-toxic anti-flu drugs from traditional Chinese medicine is a promising route. The literature reported that the use of molecular docking

✉ Peng Tan
410578772@qq.com

[1] Key Laboratory of Biological Evaluation of TCM Quality of State Administration of Traditional Chinese Medicine, Sichuan Academy of Chinese Medicine Sciences, Chengdu 610041, China

[2] Sichuan Key Laboratory for Medicinal American Cockroach, Sichuan Good Doctor Panxi Pharmaceutical Co., Ltd., Chengdu 610000, China

[3] Sichuan Engineering Research Center of Antiviral Traditional Chinese Medicine Industrialization, Pengzhou 611900, China

techniques to screen NA inhibitors from a database of herbal medicines and found that neoglucobrassicin compounds had good inhibitory activity against NA [15]. A small amount of literature also reported the use of HPLC-FLD technique to screen NA inhibitors from four herbal medicines, including *Scutellariae Radix*, *Notopterygii Rhizoma Et Radix*, *Gardeniae Fructus*, and found that chemical components such as baicalein, baicalin, and isochlorogenic acid inhibited NA activity more strongly [16]. In addition, some investigators have used UPLC–Q-TOF-MS to analyze the anti-NA activity of 27 chemical components of *Paeonia delavayi*, found that benzoylpaeoniflorin and pentagalloyl glucose had strong NA inhibitory activity [17]. However, there is a great lack of anti-flu virus activity evaluation techniques, with only a few methods such as molecular docking [18], ultrafiltration mass spectrometry [19], and cellular screening [20, 21], and there are defects such as poor accuracy, expensive instruments, and low screening efficiency, which seriously restrict the process of screening anti-influenza virus drugs from traditional Chinese medicine. Therefore, there is an urgent need to establish some assays with rapid, simple, high sensitivity and low cost characteristics for the inhibition of NA activity, and to evaluate the activity of chemical components in Chinese herbal medicines commonly used in clinical treatment of influenza, to obtain candidate compounds with strong anti-flu activity and lay the foundation for the development of new anti-flu drugs.

Experimental

Reagents and chemicals

In this study, a total of 39 high-purity compounds were purchased from Chengdu Pufeide Biotechnology company, the purity of each compound is over 98%, as validated by HPLC-DAD, The detailed information is shown in Table 1. Neuraminidase and enzyme substrates [2'-(4-methylumbelliferyl)-a-D-acetylneuraminic acid] were purchased from Shanghai Beyotime biotechnology company, and their lot numbers were 071420211105, 052119210115, 071420220117. Peramivir solution was purchased from Guangzhou nanxin pharmaceutical company, and its lot number was 3141756, the concentration was 456.8 μmol·L^{-1}. A total of 30 batches of anti-flu granules were purchased from Sichuan Good Doctor Panxi Pharmaceutical company; the lot numbers were kg01–kg30, respectively.

Apparatus

A synergy H1 Full-featured microplate testing instrument (Agilent, USA) was equipped with an autosampler and a fluorescence detector. A vortex oscillator (Beijing, China) was purchased from Dalong Xingchuang Experimental instrumental company. A SK250H ultrasonic cleaner (Shanghai, China) was purchased from Kudos Ultrasonic Instrument company. A XPE 26 Electronic balance (Mettler Toledo, Switzerland) was used for weighing samples. A milli-Q ultrapure water purifier (Millipore, USA) was used to provide the solvent. 96-well fluorescent microtiter plate was purchased from Zhejiang Beilanbo Biotechnology company, and its lot number was AD2051118.

Sample solution preparation

Accurately weighed 5 mg of each compound, dissolved in 100 μL of dimethyl sulfoxide (abbreviated as DMSO), and sonicated for 5 min as the initial concentration test solution of each compound. The initial concentration test solutions were diluted 200, 500, 1000, 10,000, 100,000 times step by step with ultrapure water, vortex shaking and ultrasonic treatment were marked as sample solutions 1, 2, 3, 4, 5, respectively, and for the final analysis. Accurately weighed 1 g of different batches of anti-flu granules, put them in a 15 mL clean test tube, added 5 mL of ultrapure water, sonicated for 5 min, accurately aspirate 1 mL diluted 10 times with ultrapure water, sonicated for 5 min, as the sample solutions of anti-flu granules, and for the final analysis.

NA standard curve preparation

First, 70 μL of NA buffer solution was added accurately to each of the six wells of the microtiter plate, followed by 0, 1, 2, 5, 7.5, and 10 μL of NA to each well. Second, a sufficient amount of ultrapure water was added to each well to bring the total solution volume to 90 μL. Third, incubated the mixed solutions at 37 °C for 2 min, added accurately 10 μL of NA fluorogenic substrate [2'-(4-methylumbelliferyl)-α-D-*N*-acetylneuraminic acid] to each mixed solution to bring the total volume of solution per well to 100 μL. The microtiter plate was shaken and mixed for 1 min, then incubated at 37 °C for 30 min. At last, the fluorescence value was detected under the conditions of excitation wavelength of 322 nm and emission wavelength of 450 nm. According to the volume of NA added and the actual detected fluorescence value, a standard curve of NA was prepared.

Sample assay

First, accurately added 70 μL of buffer solution to each well of the 96-well fluorescence microtiter plate, then added 10 μL of NA, and then added 10 μL of 5 sample solutions of different concentrations, respectively. Make sure that each concentration of the test solution was detected 3 times in parallel at the same time. After a 2-min

Table 1 Details of 39 compounds

Source	Compound	Purity/%	Batch No
Lomicrae Japonicae Flos	Chlorogenic acid	99.44	21032502
Lomicrae Japonicae Flos	Neochlorogenic acid	99.62	20123006
Lomicrae Japonicae Flos	Cryptochlorogenic acid	98.15	21061801
Lomicrae Japonicae Flos	Isochlorogenic acid A	99.61	21112405
Lomicrae Japonicae Flos	Isochlorogenic acid B	98.55	21022308
Lomicrae Japonicae Flos	Isochlorogenic acid C	99.77	21031902
Lomicrae Japonicae Flos	Methyl chlorogenate	99.52	20090706
Lomicrae Japonicae Flos	Luteoloside	99.34	20060301
Lomicrae Japonicae Flos	Luteolin	99.02	20121605
Lomicrae Japonicae Flos	Isoquercitrin	99.83	20112404
Lomicrae Japonicae Flos	Asperosaponin VI	99.88	19121901
Lomicrae Japonicae Flos	Hyperoside	98.35	19103001
Lomicrae Japonicae Flos	Mudanpioside C	99.43	20113001
Lomicrae Japonicae Flos	Loganic acid	99.36	18062502
Lomicrae Japonicae Flos	Kaempferide	98.75	21010804
Lomicrae Japonicae Flos	Rutoside	99.72	20110501
Lomicrae Japonicae Flos	Caffeic acid	98.35	21040609
Lomicrae Japonicae Flos	Quercetin	98.64	21032404
Lomicrae Japonicae Flos	Quercitrin	99.48	21012903
Lomicrae Japonicae Flos	Loganin	99.34	21032507
Lomicrae Japonicae Flos	Gallic acid	98.21	18120403
Lomicrae Japonicae Flos	Macranthoidin B	98.74	17021504
Lomicrae Japonicae Flos	1,2,3,4,6-*O*-Pentagalloylglucose	99.10	19010904
Lomicrae Japonicae Flos	Quercetin 7-*O*-β-D-glucopyranoside	99.00	17042105
Lomicrae Japonicae Flos	Veronicastroside	98.11	200630
Lomicrae Japonicae Flos	α-Hederin	98.18	18092801
Lomicrae Japonicae Flos	Hyperoside	98.05	181028
Lomicrae Japonicae Flos	2''-*O*-Galloylhyperin	98.76	200701
Paeoniae Radix Rubra	Paeoniflorin	98.20	20030901
Paeoniae Radix Rubra	Alibiflorin	99.28	19121705
Paeoniae Radix Rubra	Oxypaeoniflora	99.67	19120604
Paeoniae Radix Rubra	Benzoylpaeoniflorin	98.14	20032703
Paeoniae Radix Rubra	Galloylpaeoniflorin	98.88	201013
Paeoniae Radix Rubra	Lactiflorin	99.61	190728
Paeoniae Radix Rubra	Benzoyloxypaeoniflorin	98.64	190516
Dryopteridis Crassirhizomatis Rhizoma	Filixic acid ABA	98.77	18020505
Dryopteridis Crassirhizomatis Rhizoma	Albaspidin AA	98.34	180228
Dryopteridis Crassirhizomatis Rhizoma	Dryocrassin ABBA	98.34	200224
Dryopteridis Crassirhizomatis Rhizoma	Albaspidin AP	98.24	180228

incubation at 37 °C, 10 μL of NA fluorogenic substrate was added to each well to bring the total solution volume to 100 μL. After incubating again at 37 °C for 30 min, the fluorescence values of each well was detected at excitation wavelength of 322 nm and emission wavelength of 450 nm. Combined with the NA standard curve and formula (1), the inhibition rate of each sample solution to NA activity can be calculated. A dose–response curve was made with the concentration and inhibition rate of each sample, and its IC_{50} value could be calculated. The dose–response curve of the inhibitory effect of each batch of anti-flu granules sample solution on NA was determined by the same experimental method.

The inhibition rate of NA for each sample was calculated according to Eq. (1), where *M* represents the amount of NA still active after binding and reaction of NA with each compound, and this amount can be read from the detected fluorescence value combined with the NA standard curve. A schematic diagram of this analysis is shown in Fig. 1.

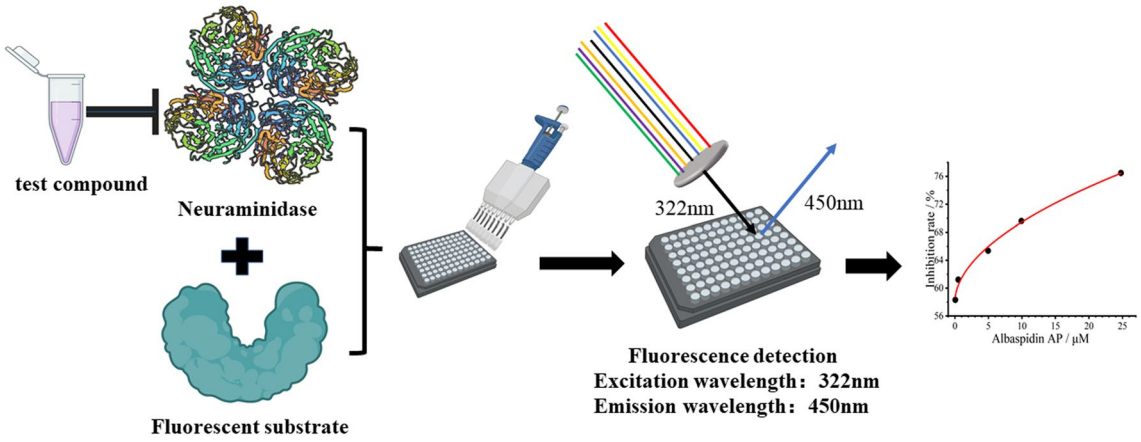

Fig. 1 Schematic diagram of the anti-NA activity screening method

$$\text{Inhibition rates } \% = (10 - M)/10 \times 100\%. \quad (1)$$

Methodological verification

The peramivir solution (228.4 μmol·L^{-1}) was used for six consecutive determinations according to the experimental method in sample assay, then the inhibition rates and RSD were calculated to evaluate the precision of the experimental apparatus. Experimenter A used peramivir solution for 6 consecutive repeated determinations between 6 days according to the experimental method in sample assay, then the inhibition rates and RSD were calculated, this was used to evaluate the inter-day precision. Experimenter B used peramivir solution for six consecutive determinations in one day according to the experimental method in sample assay, then the inhibition rates and RSD were calculated, this was used to evaluate the intra-day precision. Experimenter B accurately weighed 6 anti-flu granules samples from the same batch (batch kg01), each sample weighed approximately 1 g, then the sample solution was prepared according to the method in sample solution preparation and the fluorescence value was detected according to the method in sample assay, and the inhibition rates and RSD were calculated, and this was used to assess the reproducibility of the new method.

Verification of whether the fluorescent substrate interferes

To exclude the interference of substrate on the assay results and to demonstrate that the actual detected fluorescence values are generated by the binding of different volume amounts of neuraminidase and substrate, the following exclusion experiment was adopted: only 10 μL of fluorescent substrate and 70 μL of buffer were added to each well, supplemented with 20 μL of ultrapure water, and 6 wells were repeated in parallel to determine the fluorescence values and calculate the inhibition rate according to the analytical method in sample assay. The fluorescence values were determined according to the analytical method in sample assay, and the inhibition rates were calculated.

Verification of whether DMSO interferes

To investigate the effect of DMSO on the accuracy of the assay results, different concentrations of DMSO were prepared according to sample solution preparation, and the fluorescence values were detected according to the analytical method in sample assay, and the inhibition rate was calculated to investigate the effect of different test concentrations of DMSO on the accuracy of the assay results.

Molecular docking analysis

To verify the accuracy of the actual detected results, the theoretical calculated values of the binding energy value and Ki value of the docked NA protein receptor and the donor were also used in the experiment to reverse the accuracy of the actual detected results. The N5 (PDB: 3TI8) of the influenza A (H1N1) virus was selected as the study target [22], and the 3D structure of NA was obtained from the Protein Data Bank (www.rcsb.org). The original ligand small molecules and water molecules were removed using Pymol software, hydrogen atoms were added, and saved as pdb format files. The receptor molecule of this pdb format file is then placed in ADT software with charge and non-polar hydrogen and saved as a pdbqt format file. The 3D structures of compounds were obtained from the PubChem (https://pubchem.ncbi.nlm.nih.gov/) compound database. For compounds without 3D structures in the PubChem database, their 2D structures were drawn using ChemDraw, saved in

mol format, and converted into 3D structures using ChemBio3D. The optimal quantization was performed by MM2 force field and saved in pdb format. Next, hydrogen addition was performed in ADT software, charge was added, charge was calculated and saved as a pdbqt file for further analysis. In ADT software, the grid of ligand molecules and receptor molecules in pdbqt format file was set and Auto Grid was run to generate the image file, and finally Auto Dock was run for molecular docking operation to obtain the ligands with Inhibit constant (abbreviated as Ki) and Binding energy as reference indexes. The Binding energy value and Ki values of molecules docked with NA proteins were obtained, and the Binding energy value and Ki values of compounds were compared with those of peramivir.

Data and image processing

Standard curve and all dose–effect curves were produced by Originpro 2022 software (OriginLab Corporation, USA), and IC_{50} for NA inhibition by different compounds were calculated using GraphPad Prism 9 software (GraphPad Software, USA).

Results and discussion

Results of the methodological validation

The results of the inter-day precision validation showed that the average inhibition rate of peramivir was 85.24% with an RSD of 2.52%; the results of the intra-day precision validation showed that the average inhibition rate of peramivir was 83.89% with an RSD of 1.06%, indicating good precision of the apparatus; the results of the reproducibility validation showed that the average inhibition rate of the anti-flu granules sample solution was 69.70% with an RSD of 2.72%, indicating that the reproducibility of the method is good and can be used to evaluate the inhibitory activity of different samples against NA.

Results of fluorescent substrate interference validation

The results of the substrate interference investigation showed that the instrument was able to measure weak fluorescence value at a given detection wavelength when only fluorescent substrate was added to the test system without NA, but the difference between the fluorescence values detected after the combined action of NA and fluorescent substrate was three orders of magnitude, so the former was basically negligible, which means that the actual fluorescence values detected in the experiment were the real values generated by the actual amount of NA and the combination of fluorescent substrate.

Results of DMSO interference validation

In the process of method establishment, we focused on the effect of different concentrations of DMSO on the accuracy of the assay results. The results showed that DMSO has a weak effect in the concentration range of 1/1,000,000–5/10,000, which dictates that the test concentration of DMSO should not be too large, but considering that the sample to be tested can have a large initial assay concentration as possible, it is finally preferred to dissolve the sample to be tested in 100 µL DMSO and then dilute it step by step to a series of different test concentrations, which can reduce the effect of DMSO to an acceptable range.

Results of standard curve preparation

Through a series of tests, the regression equation of NA was produced as $Y = 12.27X + 1.47$ with r of 0.997 based on the reaction quantity of NA and the detected fluorescence value, indicating that the reaction quantity of different NA showed a good linear relationship with the fluorescence value within a certain range. Based on this linear equation, 10 µL of NA, 10 µL of sample solution and 10 µL of fluorescent substrate were added to the test system in turn, and the fluorescence value was detected after 30 min of reaction, and the amount of NA that remained active after being inhibited by the sample could be calculated based on the detected fluorescence and this linear equation, and the inhibition rate of NA by the sample could be calculated in combination with the sample assay. Based on the actual detected inhibition rates of different test concentrations of peramivir, the IC_{50} of peramivir was calculated to be 118.1 µmol·L^{-1}, as shown in Fig. 2.

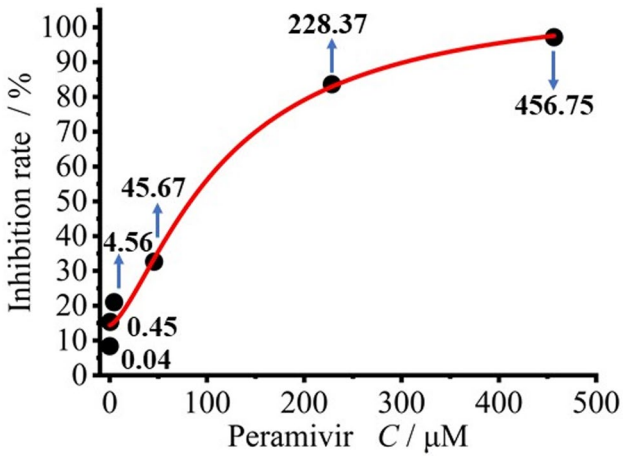

Fig. 2 Dose–effect curve formed by different test concentrations of peramivir and the corresponding inhibition rates against NA

Results of compound samples analysis

Based on the newly established anti-NA activity analytical method, in vitro anti-NA activity of 39 high-purity chemical compounds from three traditional Chinese herbal medicines commonly used in clinical treatment of influenza was screened and evaluated, and a total of 25 compounds were obtained with IC_{50} lower than that of peramivir. It is of interest to note that, in terms of the IC_{50}, the test concentration of lonicera saponin B (3.57 μmol·L^{-1}) from *Lomicrae Japonicae Flos* was about one-thirty-third of that of peramivir (118.1 μmol·L^{-1}), preliminarily indicating a strong in vitro inhibitory activity of lonicera saponin B against NA. The IC_{50}s of the remaining compounds, such as quercetin (11.82 μmol·L^{-1}), pelargonium AP (24.77 μmol·L^{-1}), honeysuckle (27.61 μmol·L^{-1}), luteolin (34.94 μmol·L^{-1}), and chlorogenic acid B (36.77 μmol·L^{-1}), were all lower than the IC_{50} of peramivir (118.1 μmol·L^{-1}), that is, preliminary indications that these compounds have stronger in vitro NA inhibitory activity than that of peramivir. The quantitative effect relationships between the actual tested concentrations and inhibition rates of the six representative compounds are shown in Fig. 3, and detailed information of 25 compounds that inhibited NA at concentrations close to IC_{50} are shown in Table 2.

Compared with the inhibitory activity of peramivir, except for the 25 chemical compounds mentioned above, the remaining 14 compounds were relatively less active in inhibiting NA in vitro. The anti-NA activity of some typical representative compounds contained in *Lomicrae Japonicae Flos* was screened and evaluated. The results showed that nine compounds, including quercetin, isochlorogenic acid A and isochlorogenic acid C, exhibited a weak inhibitory effect. In order of inhibition activity: quercetin-7-*O*-β-D-glucopyranoside (0.1 μmol·L^{-1}, 48.23%), quercetin (0.19 μmol·L^{-1}, 41.76%), isochlorogenic acid A (49.38 μmol·L^{-1}, 38.58%), isochlorogenic acid C (50.34 μmol·L^{-1}, 37.34%), caffeic acid (133.22 μmol·L^{-1}, 34.97%), neochlorogenic acid (80.44 μmol·L^{-1}, 32.76%), cryptochlorogenic acid (76.20 μmol·L^{-1}, 32.65%), 1,2,3,4,6-*O*-pentagalloylglucose (95.17 μmol·L^{-1}, 16.72%), chlorogenic acid (56.45 μmol·L^{-1}, 27.69%). The quality control indexes for *Lomicrae Japonicae Flos* in the Pharmacopoeia of the People's Republic of China (2020 edition) are chlorogenic acid, isochlorogenic acid A and isochlorogenic acid C, but the evaluation results of this experiment initially showed that these three compounds have weak inhibitory activity against NA in vitro, which also implies that these three compounds are not the best quality control indexes for *Lomicrae Japonicae Flos*. The anti-NA activity of some representative compounds contained in Paeonia

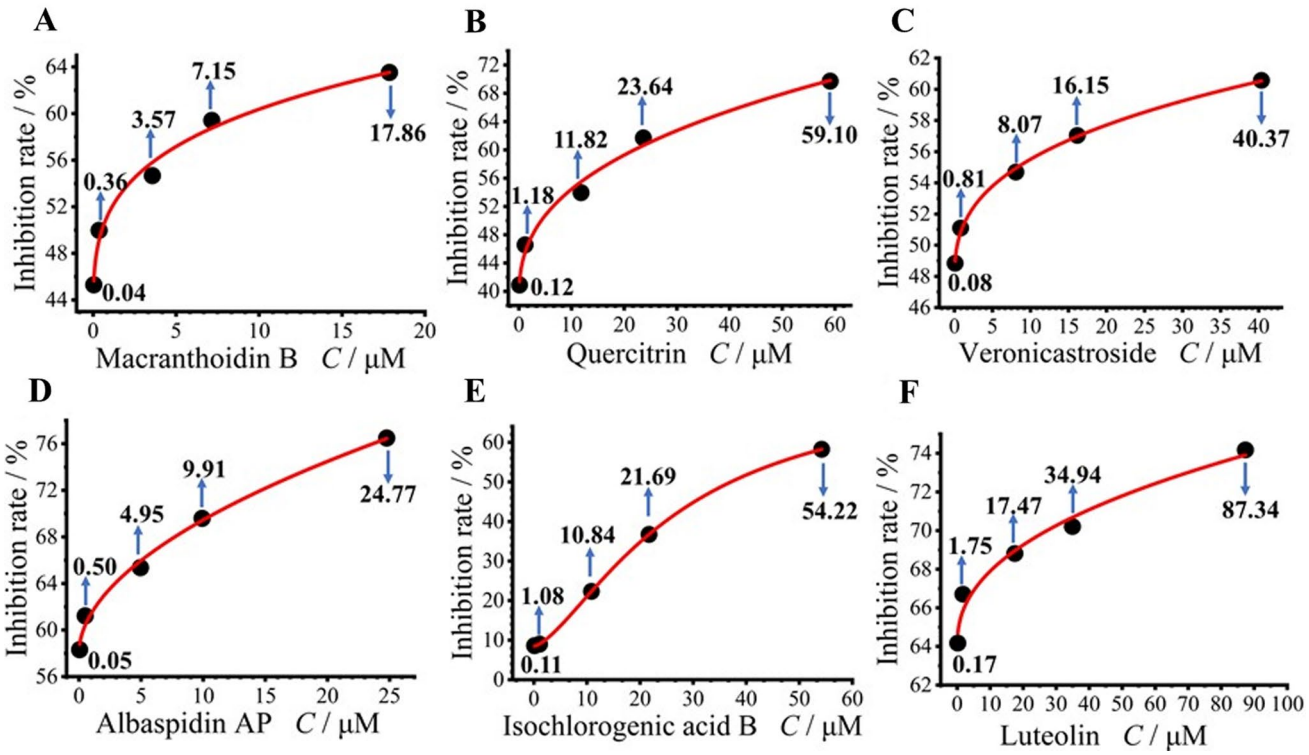

Fig. 3 Dose–effect curves formed by different test concentrations of six representative compounds with their corresponding inhibition rates against NA

Table 2 Detailed information on the 25 compounds that inhibited NA at concentrations close to 50% of the tested concentrations

Chinese herbal medicine	Compound	C/μM	Inhibition rate / %
Paeoniae Radix Rubra	Lactiflorin	0.18	53.78
Lonicerae Japonicae Flos	Macranthoidin B	3.57	54.67
Lonicerae Japonicae Flos	α-Hederin	6.92	54.45
Lonicerae Japonicae Flos	Quercitrin	11.82	53.96
Paeoniae Radix Rubra	Benzoyloxypaeoniflorin	13.99	51.75
Dryopteridis Crassirhizomatis Rhizoma	Dryocrassin ABBA	14.62	83.46
Lonicerae Japonicae Flos	Veronicastroside	16.15	57.04
Lonicerae Japonicae Flos	Macranthoidin A	18.18	58.86
Dryopteridis Crassirhizomatis Rhizoma	Filixic acid ABA	21.76	71.84
Dryopteridis Crassirhizomatis Rhizoma	Albaspidin AP	24.77	58.31
Lonicerae Japonicae Flos	Asperosaponin VI	29.06	62.79
Dryopteridis Crassirhizomatis Rhizoma	Albaspidin AA	29.67	77.15
Lonicerae Japonicae Flos	Luteolin	34.94	70.21
Lonicerae Japonicae Flos	2"-*O*-Galloylhyperin	36.50	68.83
Lonicerae Japonicae Flos	Rutoside	38.49	90.67
Lonicerae Japonicae Flos	Loganin	43.55	64.39
Lonicerae Japonicae Flos	Mudanpioside C	49.95	89.90
Lonicerae Japonicae Flos	Luteoloside	51.30	62.98
Lonicerae Japonicae Flos	Isoquercitrin	53.84	72.49
Lonicerae Japonicae Flos	Isochlorogenic acid B	54.22	58.24
Lonicerae Japonicae Flos	Hyperoside	55.99	54.87
Lonicerae Japonicae Flos	Gallic acid	64.66	81.02
Lonicerae Japonicae Flos	Kaempferide	64.94	83.99
Lonicerae Japonicae Flos	Loganic acid	71.74	85.69
Lonicerae Japonicae Flos	3-*O*-Caffeoylquinic acid methyl ester	76.02	85.78

lactiflora was screened and evaluated. Among them, compounds such as benzoylpaeoniflorin showed weak inhibitory activity. In order of inhibition activity: benzoylpaeoniflorin (50.46 μmol·L^{-1}, 41.22%), galloylpaeoniflorin (10.59 μmol·L^{-1}, 41.02%), oxypaeoniflora (22.16 μmol·L^{-1}, 39.95%), alibiflorin (49.95 μmol·L^{-1}, 33.64%), paeoniflorin (58.28 μmol·L^{-1}, 27.51%).

Results of anti-flu granules samples analyze

Based on the newly established method for the determination of anti-NA activity, the in vitro anti-NA activity of a commonly used clinical anti-flu Chinese patent medicine (anti-flu granules) was evaluated, and all 30 batches of anti-flu granules produced by the same manufacturer were collected for the determination of the overall anti-NA activity. The results showed that there were some differences in the inhibitory activities of the anti-flu granules samples from batches kg01 to kg30 against NA at all tested concentrations of 0.02 g·mL^{-1}, indicating that there were some differences in the overall quality of the anti-flu granules between the batches. Among them, kg03, kg05, kg22, kg23, kg24, kg26, kg27, kg28, kg29 and kg30 showed higher anti-NA activity, ranging from 80 to 98%, indicating good overall quality consistency among these samples. The samples kg04, kg06 and kg12 batches showed poor anti-NA activity, with inhibition rates of 30% around. Of concern was the kg20 sample, with an inhibition rate of only 49%, and the rest of the batches had inhibition rates ranging from 50 to 70%, indicating relatively poor overall quality consistency among these samples.

Results of molecular docking analysis

Spatial matching is the basis for intermolecular interactions and energy matching is the basis for maintaining stable binding between molecules, so binding energy is a key indicator for screening active molecules. The Binding energy values and Ki values of 25 ligand molecules docked with NA receptors, such as peramivir, kaempferol and lignocaine, are shown in Table 3. The results showed that the Binding energy values and Ki values of peramivir docked with NA receptors were small, − 11.80 kJ·mol^{-1} and 8.56 mmol·L^{-1}, respectively, indicating that the peramivir was spatially matched to each other and bound more

Table 3 Details of docking data of ligand compounds with NA

Chinese herbal medicine	Compound	Binging Energy/ kJ·mol^{-1}	Ki/mmol·L^{-1}
Peramivir	Peramivir	− 11.80	8.56
Lomicrae Japonicae Flos	Kaempferide	− 19.25	0.42
Lomicrae Japonicae Flos	Luteolin	− 19.20	0.43
Lomicrae Japonicae Flos	Quercitrin	− 18.16	0.66
Dryopteridis Crassirhizomatis Rhizoma	Albaspidin AP	− 17.20	0.97
Lomicrae Japonicae Flos	Luteoloside	− 17.07	1.02
Paeoniae Radix Rubra	Benzoyloxypaeoniflorin	− 16.57	1.26
Lomicrae Japonicae Flos	3-*O*-Caffeoylquinic acid methyl ester	− 15.77	1.71
Paeoniae Radix Rubra	Lactiflorin	− 15.73	1.76
Lomicrae Japonicae Flos	Gallic acid	− 15.10	2.25
Lomicrae Japonicae Flos	α-Hederin	− 13.68	4.03
Lomicrae Japonicae Flos	Loganin	− 12.43	6.63
Dryopteridis Crassirhizomatis Rhizoma	Albaspidin AA	− 11.63	9.14
Lomicrae Japonicae Flos	Mudanpioside C	− 11.05	11.6
Lomicrae Japonicae Flos	Loganic acid	− 10.92	12.15
Lomicrae Japonicae Flos	Isoquercitrin	− 10.63	13.67
Lomicrae Japonicae Flos	Isochlorogenic acid B	− 8.03	39.05
Lomicrae Japonicae Flos	Rutoside	− 7.15	55.78
Lomicrae Japonicae Flos	Hyperoside	− 6.65	68.85
Dryopteridis Crassirhizomatis Rhizoma	Filixic acid ABA	− 6.36	76.63
Lomicrae Japonicae Flos	2"-*O*-Galloylhyperin	− 4.10	190.05
Lomicrae Japonicae Flos	Veronicastroside	− 4.02	198.77
Lomicrae Japonicae Flos	Asperosaponin VI	0.50	Unavailable
Dryopteridis Crassirhizomatis Rhizoma	Dryocrassin ABBA	1.97	Unavailable
Lomicrae Japonicae Flos	Macranthoidin A	13.64	Unavailable
Lomicrae Japonicae Flos	Macranthoidin B	/*	/

*Represent that this compound failed to dock successfully with the NA protein molecule

firmly when molecularly docked with NA receptors, and showed strong virtual inhibitory activity against NA proteins (See Fig. 4a). The binding energy values of 11 compounds, including kaempferol and luteolin, were lower than those of peramivir, suggesting that these 11 compounds may have a strong virtual inhibition of NA, and the order of strength of the virtual calculations was as follows: kaempferide, luteolin, quercitrin, albaspidin AP, luteoloside, benzoyloxypaeoniflorin, methyl chlorogenate, lactiflorin, gallic acid, α-hederin, and loganin. The small Ki values indicated that these 11 compounds had strong affinity with NA receptors, indicating that they could inhibit NA at low concentrations, which was consistent with the results of the previous experiments. The binding energy value and Ki values of four compounds, including albaspidin AA and mudanpioside C, were close to those of peramivir, indicating that these four compounds had a strong virtual anti-NA activity, which was basically consistent with the results actually detected in the previous experiments. Some of the remaining compounds showed weaker virtual binding ability to NA and lower virtual anti-NA activity. A small amount of inconsistency existed between this part of the results and the previous NA activity inhibition results, which may be explained by the fact that this part of the compounds achieved NA activity inhibition by interacting with other active sites in the NA protein. The docking sites of kaempferide, luteolin, quercitrin with the receptor protein were selected for visualization (See Fig. 4), and as shown, the three compounds have binding activity to amino acid residues at multiple sites of the protein receptor, and these compounds form hydrogen bonds with the amino acids and effectively bind to the active site of NA through hydrogen bonding interactions, suggesting a possible inhibitory effect on NA activity. The binding of compounds and amino acid residues showed a multi-targeted action profile, such as peramivir (TRP-383, GLU-313, ILE-384) binding to groups such as –OH and –NH_3^+, kaempferide (ASN-247, ASN-347A, GLY-345) binding to groups such as –OH and R–O–R, luteolin (GLN-136, LYS -143) bound to –OH and other groups, and quercitrin (ASN-347A, ASN-264, GLN-265, SER-369) bound to –OH and other

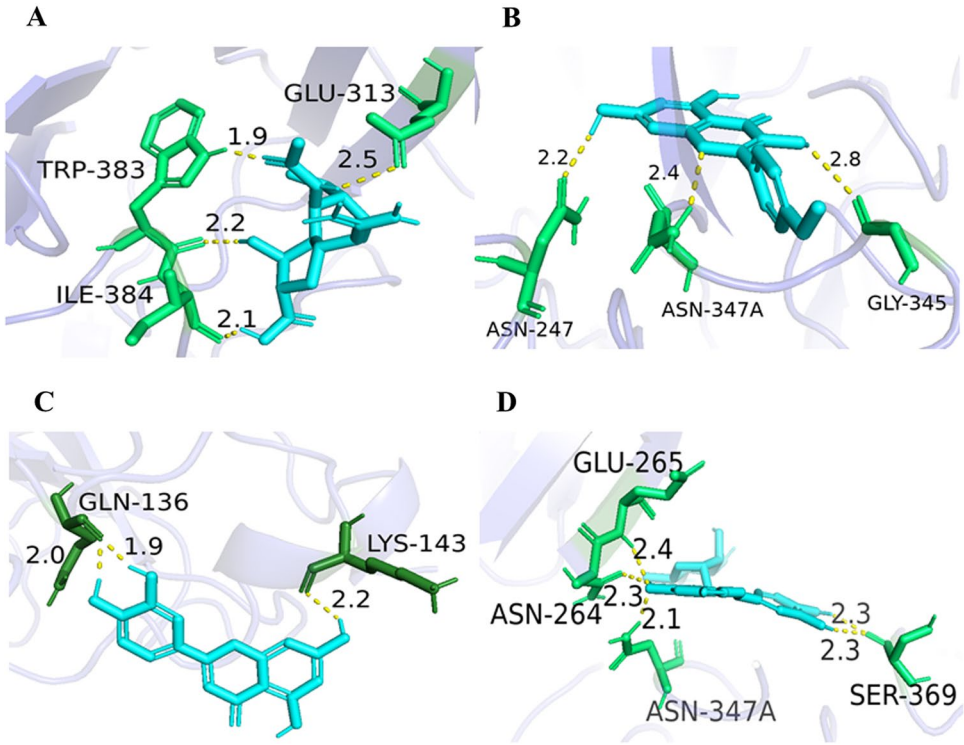

Fig. 4 Schematic diagram of the docking of amino acid residues of neuraminidase with some typical compounds. **a** peramivir; **b** kaempferide; **c** luteolin; **d** quercitrin

groups suggesting that the anti-flu herbs commonly used in clinical practice may act on multiple targets through multiple components to achieve anti-NA activity [23]. Schematic diagrams of the docking of amino acid residues of neuraminidase with some typical compounds are shown in Fig. 4, and details of the docking data of the ligand compounds with NA are shown in Table 3. The results showed that the theoretical calculated values of most of the compounds were in good agreement with the actual detected values, which means the actual detected in vitro inhibitory activities of the different compounds on neuraminidase by this method are highly accurate.

Conclusions

In this paper, a new analytical method was developed for the rapid screen and evaluation of traditional Chinese herbal medicines (including chemical components or Chinese patent medicines) for their in vitro anti-NA activity. A total of 39 compounds contained in three traditional Chinese herbal medicines were screened and evaluated for their in vitro anti-NA activity. 25 compounds were found to have strong anti-NA activity, providing candidate compounds for further development of anti-flu drugs. More importantly, this paper applies the newly established method to the quality consistency evaluation of different batches of Chinese patent medicines. By evaluating the strength of anti-NA activity in vitro, it is not necessary to analyze the drug components, determine the content level of index components, etc., but to characterize the overall strength of anti-viral activity of the drug, and to express the overall pharmacological effects of the drug in objective values, which is more in line with the characteristics of complex components and overall effects of traditional Chinese medicines. In conclusion, we initially established a practical, rapid, sensitive and low-cost screening method for influenza virus neuraminidase herbal inhibitors, but there are certain shortcomings, only in vitro activity evaluation was performed, and further in vivo validation studies are still needed.

Acknowledgements This work was supported by Sichuan Science and Technology Program (grant number 2022YFS0429, 2022YFS0431, 2022ZYD0102).

Data Availability The data that support the findings of this study are available on request from the corresponding author, [Peng Tan, Email:410578772@qq.com], upon reasonable request.

Declarations

Conflict of interest The authors have declared no conflict of interests.

References

1. C. Paules, K. Subbarao, Lancet **390**, 697 (2017)
2. T.K. Burki, Lancet. Respir. Med. **9**, e103 (2021)
3. J.C. Kwong, K.L. Schwartz, M.A. Campitelli, H. Chung, N.S. Crowcroft, T. Karnauchow, K. Katz, D.T. Ko, A.J. McGeer, D.

McNally, D.C. Richardson, L.C. Rosella, A. Simor, M. Smieja, G. Zahariadis, J.B. Gubbay, N. Engl, J. Med. **378**, 345 (2018)
4. J. Baj, H.K. Juchnowicz, G. Teresiński, G. Buszewicz, M. Ciesielka, R. Sitarz, A. Forma, K. Karakuła, W. Flieger, P. Portincasa, R. Maciejewski, J. Clin. Med. **9**, 1753 (2020)
5. C. Chaccour, A. Casellas, A.B.D. Matteo, I. Pineda, A. Fernandez-Montero, P. Ruiz-Castillo, M.A. Richardson, M. Rodríguez-Mateos, C. Jordán-Iborra, J. Brew, F. Carmona-Torre, M. Giráldez, E. Laso, J.C. Gabaldón-Figueira, C. Dobaño, G. Moncunill, J.R. Yuste, J.L.D. Pozo, N.R. Rabinovich, V. Schöning, F. Hammann, G. Reina, B. Sadaba, M. Fernández-Alonso, eClinicalMedicine **32**, 100720 (2021)
6. S.J. Tian, N. Hu, J. Lou, K. Chen, X.Q. Kang, Z.J. Xiang, H. Chen, D.L. Wang, N. Liu, D. Liu, G. Chen, Y.L. Zhang, D. Li, J.R. Li, H.X. Lian, S.M. Niu, L.X. Zhang, J.J. Zhang, J. Infect. **80**, 401 (2020)
7. L.C. Marr, J.W. Tang, J.V. Mullekom, S.S. Lakdawala, J.R. Soc, Interface **16**, 20180298 (2019)
8. M.L. Jackson, J.R. Chung, L.A. Jackson, C.H. Phillips, J. Benoit, A.S. Monto, E.T. Martin, E.A. Belongia, H.Q. McLean, M. Gaglani, K. Murthy, R. Zimmerman, M.P. Nowalk, A.M. Fry, B. Flannery, N. Engl, J. Med. **377**, 534 (2017)
9. T. Komeda, S. Ishii, Y. Itoh, Y. Ariyasu, M. Sanekata, T. Yoshikawa, J. Shimada, J. Infect. Chemother. **21**, 194 (2015)
10. H. Ono, M. Okamura, A. Fukushima, Yakugaku Zasshi **138**, 1201 (2018)
11. X.Y. Peng, Y.C. Xiao, L. Li, D.X. Wen, X.Y. Gong, B.F. Li, L.L. Zhou, Eur. J. Inflamm. **18**, 1 (2020)
12. T.F. Lau, P.C. Leung, E.L.Y. Wong, C. Fong, K.F. Cheng, S.C. Zhang, C.W.K. Lam, V. Wong, K.M. Choy, W.M. Ko, Am. J. Chin. Med. **33**, 345 (2005)
13. K.X. Chen, H.Z. Chen, Front. Med. **14**, 529 (2020)
14. M. Lyu, G.W. Fan, G.X. Xiao, T.Y. Wang, D. Xu, J. Gao, S.Q. Ge, Q.L. Li, Y.L. Ma, H. Zhang, J.G. Wang, Y.L. Cui, J.H. Zhang, Y. Zhu, B.L. Zhang, Acta. Pharm. Sin. B. **11**, 3337 (2021)
15. V. Karthick, K. Ramanathan, SpringerPlus **2**, 115 (2013)
16. G.Y. Yu, D. Fang, Int. J. Anal. Chem. **2021**, 6694771 (2021)
17. J.H. Li, X.Y. Yang, L.F. Huang, Molecules **21**, 1133 (2016)
18. H. Patel, A. Kukol, Drug. Discov. Today. **26**, 503 (2021)
19. C.X. Cao, P.X. Du, X.M. Zhu, H.J. Yan, X.Y. Song, H. Zhu, Y.L. Geng, D.J. Wang, J. Sep. Sci. **42**, 2621 (2019)
20. J.W. Liu, M. Zu, K.T. Chen, L. Gao, H. Min, W.L. Zhuo, W.W. Chen, A.L. Liu, BMC. Complement. Altern. Med. **18**, 102 (2018)
21. J.J. Zhang, T. Liu, X.M. Tong, G. Li, J.H. Yan, X. Ye, Antiviral. Res. **93**, 48 (2012)
22. C.J. Vavricka, Q. Li, Y. Wu, J.X. Qi, M.Y. Wang, Y. Liu, F. Gao, J. Liu, E.G. Feng, J.H. He, J.F. Wang, H. Liu, H.L. Jiang, G.F. Gao, Plos. Pathog. **7**, e1002249 (2011)
23. H.X. Ai, X.W. Wu, M.Y. Qi, L. Zhang, H. Hu, Q. Zhao, J. Zhao, H.S. Liu, Interdiscip. Sci. **10**, 320 (2018)